Two-Dimensional Needle Growth of Electrodeposited Ni on Reconstructed Au(111)

F. A. Möller, O. M. Magnussen, and R. J. Behm
Abteilung Oberflächenchemie und Katalyse, Universität Ulm, D-89069 Ulm, Germany
(Received 22 July 1996)

In situ scanning tunneling microscopy experiments reveal a new growth morphology in the form of highly anisotropic monolayer islands (needles) during the electrodeposition of submonolayer coverages of Ni on reconstructed Au(111). To explain the well-defined orientation and shape of these Ni needles a model is suggested where the interaction with the underlying substrate lattice induces a pronounced structural anisotropy in the Ni deposit. The unusual nucleation and growth behavior allows the generation of novel Ni nanogratings. [S0031-9007(96)01327-0]

PACS numbers: 68.35.Bs, 61.16.Ch, 68.55.Jk, 81.15.Pq

The formation of nanometer scale structures by deposition of submonolayer amounts is a nonequilibrium process, which is controlled by the deposition conditions. The shape of such structures depends mainly on the diffusion of adatoms across the surface and along the edges of already existing deposits and hence is influenced strongly by the substrate symmetry. On surfaces with hexagonal lattices compact islands, randomly ramnified aggregates, and dendrites have been found [1–3]. In contrast, extremely anisotropic, needlelike structures usually require a pronounced effective anisotropy [4] and are observed only on substrates with considerable lattice anisotropy such as fcc (110) surfaces [2]. Here we present scanning tunneling microscopy (STM) results showing needle growth of electrodeposited Ni on reconstructed Au(111). The atoms in the surface layer of the reconstructed Au(111) substrate are contracted uniaxially by 4.5% along the $[1\bar{1}0]$ direction [5] and the surface anisotropy is consequently very small ($\approx$3% difference in spacing between the nearest- and next-nearest neighbor atoms). A strongly anisotropic growth of a simple metallic adsorbate is therefore highly unusual. To explain this phenomenon we suggest a model where the needle growth is caused by a structural anisotropy in the Ni deposit, namely, a uniaxial contraction induced by the underlying reconstructed Au lattice.

The homebuilt electrochemical STM used in the experiments and the experimental procedures are described in detail in Ref. [6]. Modified Watts electrolyte ($10^{-2}M$ H_3BO_3, $10^{-4}M$ HCl, and $10^{-3}M$ $NiSO_4$), prepared from suprapure H_3BO_3, suprapure HCl, p.a. grade $NiSO_4$ and Milli-Q water, and freshly flame annealed Au(111) sample were used. The sample was immersed at -0.2 V with the potentials of sample and tip controlled potentiostatically versus an Ag/AgCl (KCl sat.) reference electrode. At this and at lower sample potentials the herringbone reconstruction of the Au surface is preserved [7]. STM images were obtained in constant current mode with the tip potential usually kept 50–100 mV below the sample potential.

As described in detail elsewhere [7,8], Ni deposition on top of the Au(111) surface commences at a potential of about -0.60 V, with nucleation at defect sites (elbows and U connections) of the Au reconstruction starting at slightly higher potentials (≤ -0.60 V) than nucleation at steps of the Au substrate (≤ -0.62 V). The typical morphology of a Au(111) surface covered with submonolayer amounts of Ni, after deposition at -0.62 V, is shown in Fig. 1. Several monatomic Ni islands with an average height of 1.7 Å can be seen on an atomically flat Au terrace. On the bare Au surface in the center of the image the characteristic double rows of the Au(111) reconstruction [5], arranged in a zigzag pattern ("herringbone"), are still visible. Two types of Ni islands can be distinguished: compact, often triangular shaped islands and strongly anisotropic, needlelike islands (arrows). The most obvious feature of the compact islands is a pronounced, $\approx$0.6 Å high, long-range modulation ("white dots"). From atomic-scale observations, which reveal a hexagonal lattice with a next-neighbor spacing of 2.50 Å and the same orientation as the Au substrate lattice, this modulation can be shown to originate from the mismatch between the hexagonal lattices of substrate and adlayer (moiré pattern) [8]. Hence, the atomic arrangement in these islands is similar as in the (111) plane of bulk Ni. The preferred orientation of the island steps corresponds to the close-packed direction of the Ni lattice.

Much more unusual is the growth of needlelike monolayer islands, examples of which are marked by arrows in Fig. 1. These needles are usually less than 40 Å wide but reach lengths of several hundred Å. Their height is 1.4 Å, which is close to the minimal height of the compact islands. The steps of the needles are very smooth along the longitudinal direction, and often seem to consist of a single, kink-free, atomic row. The orientation of the needle islands is strictly determined by the local orientation of the Au(111) reconstruction. The needles run always perpendicular to the double rows of the reconstruction, i.e., along the $[1\bar{1}0]$ direction, where the topmost Au layer is 4.5% contracted. If a needle approaches a reconstruction domain of different orientation, as, e.g., in the lower left corner of Fig. 1, it stops growing. In no case was a change in orientation or even ramnification of the needles observed.

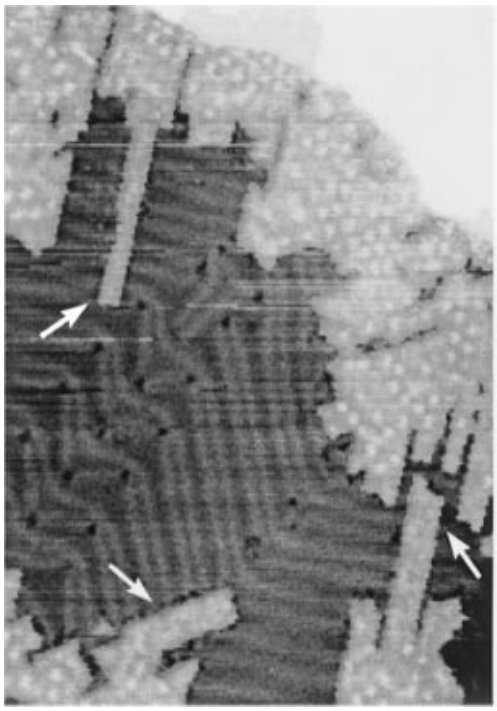

FIG. 1. STM image showing the morphology of Ni submonolayer coverages electrodeposited at -0.62 V on reconstructed Au(111) ($I_t = 4$ nA, 550×840 Å^2). Beside Ni monolyaer islands with compact shapes, needlelike deposits are visible (arrows).

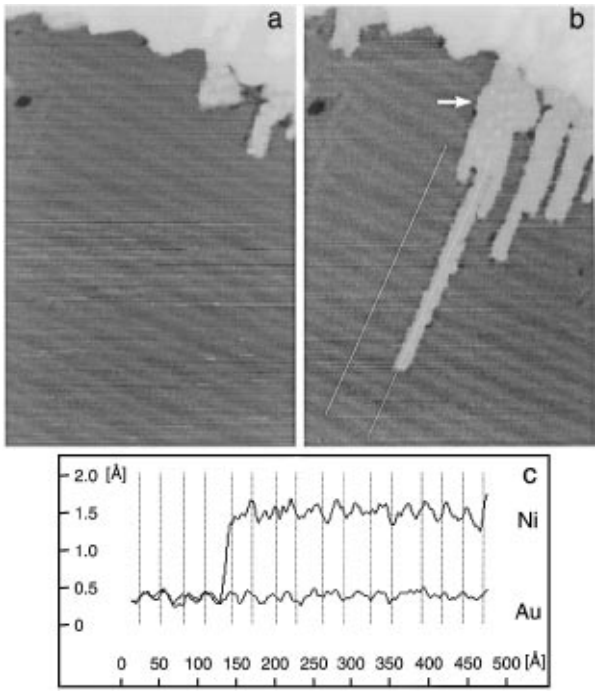

FIG. 2. STM images showing the growth of Ni monolayer needles on reconstructed Au(111) ($I_t = 4$ nA, 520×760 Å^2). (a) After a potential change to -0.63 V nuclei of the needle islands start growing. (b) Image recorded successively at a potential of -0.6 V. (c) Parallel cuts along the lines indicated in (b).

The growth of these needle islands can be directly observed in Fig. 2. Figure 2(a) shows a single reconstruction domain on a Au terrace 3 min after a potential change from -0.59 to -0.63 V. At this potential Ni nucleates predominantly at the Au steps, causing the formation of several small Ni islands at the lower edge of the Au step in the upper part of the image [7]. One of these islands exhibits a rectangular shape and can hence be identified as a needle in the initial stages of growth. At the beginning of the subsequently recorded image [Fig. 2(b)] the potential was changed back to -0.60 V to slow down the growth of the Ni islands. Nevertheless, the islands have already evolved to pronounced, parallel needles, with the longest one extending 500 Å into the terrace. Figure 2(b) suggests that the widths of the needles are not randomly distributed but that certain ("magic") values are preferred. An analysis of about 30 different needles indicates that these magic widths are $n(11.5 \pm 1.0$ Å) with $n \leq 4$. Although the needles grow predominantly in the longitudinal direction, thickening of the islands is possible by two mechanisms: either by nucleation and growth of single additional atomic rows along the needle edge [arrow in Fig. 2(b)] or by the parallel growth of a directly neighbored second needle, consisting of several atomic rows (to the right of the longest needle). In the latter case the shape of the added needle is preserved; i.e., the growing island maintains a constant width up to the needle tip during the growth. For thicknesses exceeding $\approx$50 Å (or $n \approx 4$), however, the needles transform into islands of the compact type, which can be observed in the upmost part of the needles in Fig. 2(b), where the typical white dots of the corresponding moiré pattern have emerged. The structural instability of wider needles may indicate that the needles are stabilized by the island edges.

From these observations we can directly conclude on the kinetics of the growth process and on the corresponding structural properties of the needles. The growth of Ni islands proceeds via deposition of Ni adatoms and their subsequent diffusion across the surface until they are attached at a Ni step edge. Even for the slightly anisotropic surface diffusion expected on reconstructed Au(111) considerably more adatoms should arrive at one of the long steps along the needle than at the needle tip. Hence, predominant growth along the needle direction is possible only if the probability to nucleate a new row of atoms is much higher at the steps forming the needle tip than at the steps along the needle. In other words, the adatom mobility along the latter steps has to be considerably higher and most of the impinging adatoms are hence transported along these steps to the needle tips, supplying the growth in needle direction. The differences in edge diffusion indicate distinct structural differences between steps along the needle and at the needle tip (see below).

As visible in Figs. 1(a) and 2(b), the needle islands do not exhibit the pronounced modulation pattern found on the compact islands, indicating a different atomic structure of the two island types. Atomic-resolution STM images of the needles, which would allow one to prove this idea

directly, could not be obtained up to now due to experimental difficulties (narrow island width, low tip stability due to H_2 evolution). However, a weak long-range modulation can be detected on the needles, which clearly differs from the moiré pattern on the compact islands and allows conclusions on the atomic structure. To show this modulation more clearly, a surface profile running along the center of the longest needle in Fig. 2(b) (Ni) is presented in Fig. 2(c). For comparison, Fig. 2(c) also shows a profile of the neighboring Au substrate surface (Au). In both profiles the typical vertical modulation of the Au reconstruction with 63 Å spacing between pairs of rows and $\approx$20 Å spacing between the rows of one pair [5] is discernible (0.2–0.3 Å corrugation amplitude). Furthermore, in both profiles the maxima are found at the same position, i.e., the double rows of the Au reconstruction appear to continue on the Ni needles. Finally, close inspection of the images reveals a long-range lateral displacement of the edge along the two needle steps (amplitude $\approx$1 Å), which reflects the lateral displacement of the Au atoms along $[1\bar{1}0]$ in the unit cell of the reconstruction [5]. These observations can be explained in two scenarios, which differ only with respect to the underlying Au lattice but not with respect to the lateral arrangement of the Ni atoms: in the first one the underlying Au surface layer is reconstructed and the Ni atoms in the needle have the same spacing as the Au surface atoms (at least along $[1\bar{1}0]$; see below); i.e., the Au reconstruction is maintained. In the second one the Au reconstruction is lifted by the Ni deposit but the Ni atoms attain a lattice spacing, which mimics the former reconstructed Au layer. The latter model seems less likely in view of the good alignment of the modulation maxima on Au and on the Ni needle as well as due to the considerably smaller Ni spacing observed in the compact islands, which should be preferred also in the needle structure. We therefore plausibly assume that the Ni needles grow on top of the reconstructed Au substrate, without rearranging the Au surface atoms.

Possible models for the atomic arrangement in the needle islands are illustrated in Fig. 3. (For simplicity the Au lattice is depicted as unmodulated and uniformly contracted along $[1\bar{1}0]$.) At a first glance a pseudomorphic structure with all Ni atoms placed in threefold-hollow sites of the reconstructed Au surface appears most obvious (model A). However, this model fails to explain the characteristic features of the Ni needles and, in particular, does not provide an apparent driving force for the extremely anisotropic growth. As indicated above, a major structural difference between the steps forming the tip and the steps along the needle is required to explain needle growth. For a pseudomorphic structure one might attribute this difference to the 0.1 Å different spacing of the Ni atoms along the two types of steps, caused by the contraction within the reconstructed Au surface layer. However, this effect should be more than compensated by the well-known structural difference of opposite step edges, which form (111) and (100) microfacets, respectively (see Fig. 3). The difference in free energy and edge mobility between these two facets [3,9] also causes the triagonal, rather than hexagonal, shape of the compact Ni islands. In addition, the pseudomorphic structure should easily adapt to changes in the orientation of the reconstruction. This should result in changes of the needle direction at the domain boundaries of the reconstruction, which was never observed. Finally, the model completely fails to explain the preference for certain magic widths of the needles.

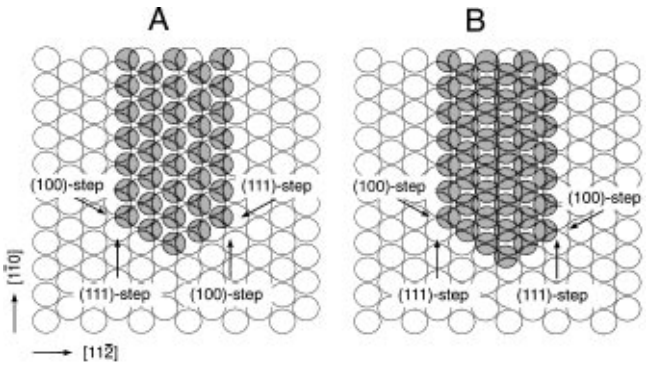

FIG. 3. Two alternative models illustrating the potential arrangement of Ni atoms (shaded circles) on the Au surface lattice (open circles) in the needles for a pseudomorphic (A) and a uniaxially contracted (B) structure.

In search for alternative structures all models with a different atomic spacing along the needle direction can be eliminated, since this would cause an additional long-range modulation pattern. The only remaining possibility is a uniaxial contraction of the Ni lattice perpendicular to the needle, i.e., along the $[11\bar{2}]$ direction of the Au lattice. Such uniaxial contracted metal adlayer structures have been observed in electrochemical environment [10] as well as under UHV conditions [11] and result from the tendency of the adlayer to improve the packing density and simultaneously avoid occupation of the energetically unfavorable top sites. A pronounced influence of the uniaxial contraction on the growth morphology, however, has not been reported up to now. In model B in Fig. 3 a uniaxial contraction to a nearest-neighbor Ni distance of 2.50 Å, the Ni spacing in the compact islands, was assumed, corresponding to a unit cell vector along $[11\bar{2}]$ of $5(\sqrt{3}/2)a_{\mathrm{Au}} \approx 12.5$ Å (with $a_{\mathrm{Au}} = 2.885$ Å). Since the Ni atoms occupy various sites from bridge to hollow sites on the Au surface, a weak modulation perpendicular to the needle direction should result (with 0.15 Å amplitude according to a ball model). Although the observation of this effect is usually complicated by the step broadening caused by the finite size of the STM tip, some of the wider needles seem to exhibit a shallow minimum along the center, which may correspond to this modulation. As can be seen in Fig. 3 needles with the magic width in this model have (111) microfacet steps along both sides while the steps at the tip both are close to (100) facets. Hence, both the pronounced anisotropy as well as the

occurrence of magic widths can be explained by this model. Since the growth anisotropy in this model is related to the intrinsic structure of the needle rather than to the substrate surface structure, the absence of changes in needle direction also is not surprising. It is noteworthy that the anisotropic islands observed during homoepitaxial growth of Au on reconstructed Au(100), where, however, the substrate anisotropy is much stronger, were explained by a very similar model [12]. The orientation of the needles is determined by the anisotropy of the reconstructed Au substrate, which provides three close-packed directions with slightly different atomic spacings. Our results indicate that the contraction of the Ni needles always occurs along the uncontracted $[11\bar{2}]$ direction of the reconstructed Au surface layer, i.e., along the direction where the interatomic distance of pseudomorphically arranged Ni atoms would be maximal.

The growth of Ni needles on Au(111) seems to be restricted to the electrochemical environment. STM studies of vapor deposited Ni on reconstructed Au(111) surfaces in UHV only find compact Ni islands, of apparently pseudomorphic structure [13]. This difference may be caused by the negative deposition potential for Ni electrodeposition, which is well below the potential of hydrogen adsorption on Ni, so that the Ni layer is covered by a H adlayer, and by the corresponding negative surface charge. The H adsorbate may weaken the bond of the Ni with the Au substrate, which is a general and well-known tendency for H adsorption [14]. H adsorption may hence lower the tendency of the Ni atoms to occupy the energetically preferred hollow sites in a pseudomorphic arrangement. In addition, hydrogen adsorption at the edges might further increase the stability of the needle steps.

By utilizing the well-defined Ni island arrays, which can be formed by deposition at -0.6 to -0.62 V on the herringbone reconstructed Au(111) surface [7], the needles can be assembled into defined periodic nanostructures. This is illustrated in Fig. 4, which was recorded directly after needle growth was initiated by a potential step from -0.62 to -0.64 V. Since the islands grow rapidly and continuously during the recording of the image, the local coverage increases from top to bottom, reflecting the increasing deposition time. The domains of the underlying Au reconstruction form a regular zigzag pattern and the Ni nuclei are localized at well-defined positions (elbows) of this pattern. Hence, the starting points as well as the growth directions of the needles are also well defined and a regular arrangement of needles (or troughs between needles) results. Because of the proceeding growth this regular pattern is discernible only locally. However, by optimizing this procedure, e.g., by stabilizing the needle growth at potentials <-0.6 V after short-time deposition at -0.64 V, well-ordered herringbone gratings formed by Ni monolayer needles with potentially unusual chemical and magnetic properties may be created.

FIG. 4. Ni nanogratings on herringbone reconstructed Au(111) formed by nucleation at -0.62 V followed by a change to -0.64 V at the upper edge of the image ($I_t = 10$ nA, 1420×1130 Å^2).

In summary, we have observed an unsuspected two-dimensional needle growth during Ni electrodeposition on Au(111). The needlelike island shape is explained by a structural anisotropy in the Ni deposit itself, namely, a uniaxial contraction across the needle caused by epitaxial effects, whereas the orientation of the needles is determined by the weak anisotropy of the reconstructed surface layer. The unusual nucleation and growth behavior of this system may be utilized for the generation of regular Ni nanogratings.

[1] C. Günther, S. Günther, E. Kopatzki, R. Q. Hwang, J. Schröder, J. Vrijmoeth, and R. J. Behm, Ber. Bunsen-Ges. Phys. Chem. **97**, 522 (1993).
[2] H. Röder, E. Hahn, H. Brune, J.-P. Bucher, and K. Kern, Nature (London) **366**, 141 (1993).
[3] T. Michely, M. Hohage, M. Bott, and G. Comsa, Phys. Rev. Lett. **70**, 3943 (1993).
[4] J. Kertész and T. Vicsek, J. Phys. A **19**, L257 (1986).
[5] J. V. Barth, H. Brune, G. Ertl, and R. J. Behm, Phys. Rev. B **42**, 9307 (1990).
[6] O. M. Magnussen, J. Hotlos, G. Beitel, D. M. Kolb, and R. J. Behm, J. Vac. Sci. Technol. B **9**, 969 (1991).
[7] F. Möller, O. M. Magnussen, and R. J. Behm (to be published).
[8] F. Möller, J. Kintrup, A. Lachenwitzer, O. M. Magnussen, and R. J. Behm (unpublished)
[9] R. Q. Hwang, J. Günther, J. Schröder, S. Günther, E. Kopatzki, and R. J. Behm, J. Vac. Sci. Technol. A **10**, 1970 (1992).
[10] J. Wang, G. M. Watson, and B. M. Ocko, Physica (Amsterdam) **200A**, 679 (1993).
[11] C. Günther, J. Vrijmoeth, R. Q. Hwang, and R. J. Behm, Phys. Rev. Lett. **74**, 754 (1995).
[12] S. Günther, E. Kopatzki, M. C. Bartelt, J. W. Evans, and R. J. Behm, Phys. Rev. Lett. **73**, 553 (1994).
[13] D. D. Chambliss, S. Chiang, and R. J. Wilson, Mater. Res. Soc. Symp. Proc. **229**, 15 (1991).
[14] K. Christmann, Surf. Sci. Rep. **9**, 1 (1988).